

# Multivariable Coupled Control of a Static Var Compensator to Improve the Power Factor of a Steel Plant with an Electric Arc Furnace Load

J.J. Marulanda-Durango, A. Escobar-Mejía, E. Giraldo

**Abstract**—In this article, a multivariable coupled control technique based in a polynomial approach is proposed over a distribution system, which includes an static var compensator (SVC), and an electric arc furnace (EAF) as a load. A multivariable step ahead coupled control structure is proposed based on an off-line identification of the multivariable system by using an Auto Regressive Moving Average (ARMA) model. The proposed controller is also evaluated over a coupled two inputs two output system where the reference is tracked in one sample. In the distribution system with the EAF load, the 3-phase voltage-current angles are defined as the outputs of the system and the 3-phase firing angles of the thyristor of the SVC are defined as the inputs of the system. The control objective is defined in order to improve the power factor (PF) of the system. A comparison analysis is performed by considering two classical approaches: a classical control strategy based on susceptances calculation, and an active power filter (APF). With the proposed method, the PF increases by 2.9% more than with the classical susceptances control. As a result, an improvement of the PF is obtained for the proposed multivariable coupled polynomial control in contrast with the classical approaches.

**Index Terms**—Multivariable coupled control, electric arc, susceptances control.

## I. INTRODUCTION

THE multivariable coupled control is a complex task that requires a complete knowledge of the system to be controlled, including the inputs-outputs dynamics [1]–[3]. Power quality problems in electrical power systems are examples of these complex systems [4]–[8].

In recent years, different strategies have been proposed to solve severe power quality problems in electrical networks, such as large consumption of reactive power, low power factor, harmonic distortion, load unbalance, voltage fluctuation, among others [9]. One of the main reason for power quality problems in distribution systems is the increase of unbalance, nonlinear, an unpredictable loads such as electric arc furnaces (EAFs) [10]. This type of load is used in the steelmaking industry to melt metallic scrap and refining

metals at high efficiencies and low operating cost [11]. However, due to the stochastic nature of the EAF operation, random variation of the reactive power and non stationary behavior of the voltage and current, is observed in this type of load, which cause considerable impact on the power quality in the upstream loads near of the EAF in the same distribution system [12]. Therefore, it is necessary to develop compensation systems in order to mitigate these and other PQ issues.

One of the custom power devices employed to counteract the effects of nonlinear loads (e.g., EAF) in power systems is the SVC. An SVC is composed by a thyristor-controlled reactor (TCR), capacitors bank, and passive filters. It is well known that the SVC provides reactive power compensation by controlling the switching angles of the thyristors [13]. Although the SVC achieves good results to improve some problems relate to PQ, the performance of SVC in reduce the flicker effects is limited to the inherent delays in the reactive power calculation in its control system [13], [14]. As a result, studies indicate that improvements about this limitation are possible [13]–[15].

Some studies propose different methods to improve the SVC performance and to mitigate the effects of EAFs on electric power systems. Most widely-used methodologies are based on the reactive power prediction of the EAF to compensate the flicker. In [15], a technique was proposed for the prediction of EAF in a stochastic model of EAF reactive power at an SVC bus, this technique uses data collected from eight arc furnaces. In [12], the reactive power calculation was obtained by combining two methods: the differential equation presented in [16] and the technique proposed in [15]. As a result, the control systems of the SVC can follow suddenly load changes to mitigate flickers. On the other hand, an integrated electric arc model was developed in [10] to predict and simulate the impact of the EAF on the electric power system. In this model, the compensation of the power factor is carried out by resonant filters and TCR to get an SVC compensator, with a control strategy based on the compensation of all negative sequence currents and the imaginary part of the positive sequence currents given by the EAF. In addition, a probabilistic prediction approach to model half-cycle ahead the reactive power consumption of an EAF was proposed in [13]. This approach used a method based on the krill herd algorithm to adjust the parameters of a support vector regression to model the uncertainty effect in the reactive power prediction. However, the aforementioned methods do not considered an improvement in the power factor as an objective in the control strategy, which is a common approach in power quality designs. In addition,

Manuscript received August 18, 2020; revised November 18, 2020. This work is carried out under the funding of the Universidad Tecnológica de Pereira, Vicerrectoría de Investigación, Innovación y Extensión. Research project: 6-20-7 “Estimación Dinámica de estados en sistemas multivariables acoplados a gran escala”.

J.J. Marulanda-Durango is an associate professor at the Department of Electrical Engineering, Universidad Tecnológica de Pereira, Pereira, Colombia, e-mail: jjmarulanda@utp.edu.co.

A. Escobar-Mejía is a full professor at the graduate and undergraduate Department of Electrical Engineering, Universidad Tecnológica de Pereira, Pereira, Colombia. Research group in Power Electronics, e-mail: andreses1@utp.edu.co.

E. Giraldo is a full professor at the Department of Electrical Engineering, Universidad Tecnológica de Pereira, Pereira, Colombia. Research Group in Automatic Control, e-mail: egiraldos@utp.edu.co.

the methods discussed above required, in almost all the cases, a detailed knowledge of the system, which not always is available. Therefore, a control approach that improves the power factor and where the controller parameters are computed considering a data-based identified model must be designed.

In this work, a multivariable coupled control technique based on a polynomial approach is proposed over a distribution system including an EAF as load, and an SVC in order to compensate the power factor as a control objective. To this end, a multivariable one step-ahead coupled control structure is proposed based on an off-line identification of the multivariable system by using an ARMA model, where the system to be controlled is identified directly from measurements. The controller is evaluated over a two inputs two outputs system in terms of tracking time-varying references. In the distribution system with the EAF load, the three-phase voltage-current angles are defined as the outputs of the system and the firing angles of the thyristor are defined as the inputs of the system. The control objective is defined to improve the PF of the system. A comparison analysis is performed by considering a two classical approaches: a control strategy based on susceptances calculation and an APF. As a result, an improvement of the PF is obtained for the proposed multivariable coupled polynomial control in contrast with the classical approaches. This paper is organized as follows: in section II the dynamical model of the distribution system with an EAF load is presented, in section III the multivariable coupled polynomial control based on a one step ahead structure is introduced, finally, in section V the comparison analysis of the proposed approach and the classical approaches in terms of the PF is given.

## II. DISTRIBUTION SYSTEM WITH ELECTRIC ARC FURNACE

The single-line diagram of the electrical distribution system feeding a steel plant is illustrated in Fig. 1. The steel plant is fed by a high-voltage line and the EAF is connected to the utility through transformers  $T_1$  (High-Voltage/Medium-Voltage) and  $T_2$  (Medium-Voltage/Low-Voltage) as shown. The utility is modeled as its Thevenin equivalent (stiff voltage source in series with a RL impedance). At the medium voltage bus, the series reactor  $X_L$  is placed to provide damping when the EAF operates, and capacitors bank are used to inject reactive power as needed. Notice that a SVC has been included at the capacitor bus. This transformer has a tap changer at the secondary side in order to adjust the furnace input voltage. The parameters of the electrical circuit used in this paper, are given in the Appendix.

In this work the electric arc model based on the energy conservation principle proposed in [17] is used. The relationship between the electric arc current  $i$  and the radius of the electric arc  $r$ , is given by the following non-linear differential equation:

$$k_1 r^2 + k_2 r \frac{dr}{dt} = \frac{k_3}{r^2} i \quad (1)$$

where  $k_1$ ,  $k_2$  and  $k_3$  are setting-parameters used to adjust the model according to the real measurements of voltage and current. The electric arc voltage  $v$  is given by

$$v = \frac{k_3}{r^2} i \quad (2)$$

The chaotic behaviour of the electric arc is produced by the amplitude modulation of  $v$  with a low frequency chaotic signal generated by the Chua's circuit, whose equations are given by [18], [19]:

$$\begin{aligned} \frac{dx}{dt} &= \begin{cases} \frac{G}{C_1} y - \frac{G + G_b}{C_1} x - \frac{G_b - G_a}{C_1} E, & \text{if } x < -E \\ \frac{G}{C_1} y - \frac{G + G_a}{C_1} x, & \text{if } -E \leq x \leq E \\ \frac{G}{C_1} y - \frac{G + G_b}{C_1} x - \frac{G_a - G_b}{C_1} E & \text{if } x > E \end{cases} \\ \frac{dy}{dt} &= \frac{1}{C_2} z - \frac{G}{C_2} (y - x) \\ \frac{dz}{dt} &= -\frac{1}{L} y \end{aligned} \quad (3)$$

where  $x(t)$ ,  $y(t)$  and  $z(t)$  are the state variables. The modulated signal is the electric arc voltage and is referred as  $v_{arc}(t)$ ,

$$v_{arc} = v(1 + wx), \quad (4)$$

where  $w$  is the gain factor of  $x(t)$  that is related with the severity of the voltage fluctuations caused by arc length variation [20]. Detailed implementation of the electric arc model used in this work is found in [21], [22] for the interested reader.

The SVC comprises a thyristor controlled reactor (TCR), and a 100 MVAR fixed capacitor bank, which makes the line currents to lead the fundamental-frequency phase-voltages at the point of common coupling (PCC). Through the TCR is possible to control the reactive power absorbed by the inductor  $L$  at the fundamental frequency, by the variation of the firing angle of the thyristors. The reactive power of the TCR (with a maximum capacity of 40 MVAR) can be adjusted modifying the firing angle of the thyristor [10] as follows:

$$Q_{TCR} = \frac{V^2}{\omega L} [2(\pi - \alpha) + \sin(2\alpha)] \quad (5)$$

where  $\alpha$  is the firing angle varying from  $\pi/2$  to  $\pi$ ,  $V$  is the root mean squared (RMS) phase voltage where the SVC is connected, and  $\omega$  is the fundamental frequency. Notice that the reactive power  $Q_{TCR}$  can be expressed as:

$$Q_{TCR} = V^2 \cdot B_{TCR} \quad (6)$$

where  $B_{TCR}$  represent the susceptance of the TCR at the fundamental frequency, which depends of the firing angle. The relationship between both  $B_{TCR}$  and  $\alpha$  is given by

$$B_{TCR}(\alpha) = \frac{2(\pi - \alpha) + \sin(2\alpha)}{\omega L} \quad (7)$$

In [17], the susceptances between phases of the SVC (the equivalent susceptance of the TCR and the filters) are computed using the symmetrical components method applied to the line currents. This method establish that the values

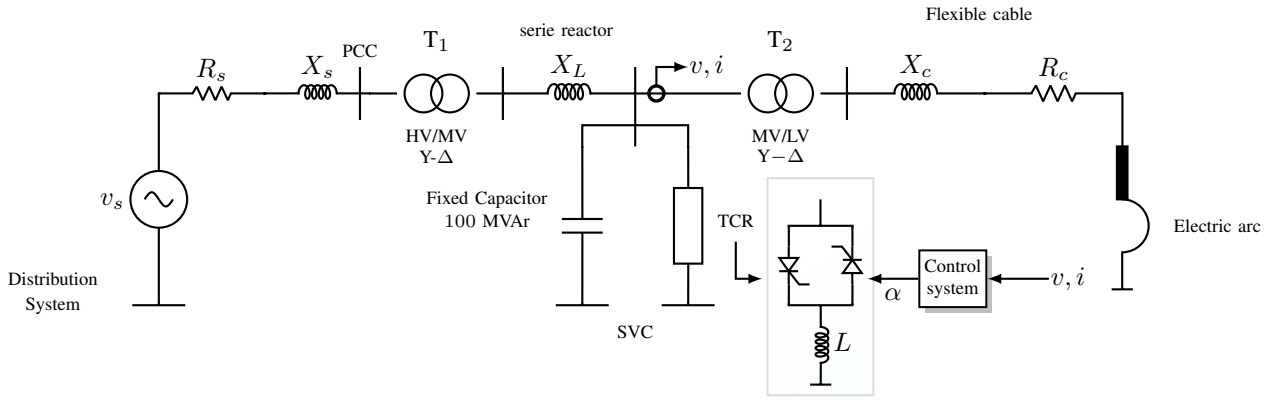


Fig. 1. Single phase block diagram of the distribution system including the electric arc furnace plant and the controller.

of the line susceptances of the SVC, that compensate the imaginary sequence component and all the negative sequence component of the arc furnace's three-phase currents, are given by

$$\begin{aligned} B_{SVC,ab} &= -\frac{1}{3\sqrt{3}V} \left( \text{Im}[\mathbb{I}_L^+] + \text{Im}[\mathbb{I}_L^-] - \sqrt{3}\text{Re}[\mathbb{I}_L^-] \right) \\ B_{SVC,bc} &= -\frac{1}{3\sqrt{3}V} \left( \text{Im}[\mathbb{I}_L^+] - 2\text{Im}[\mathbb{I}_L^-] \right) \\ B_{SVC,ca} &= -\frac{1}{3\sqrt{3}V} \left( \text{Im}[\mathbb{I}_L^+] + 2\text{Im}[\mathbb{I}_L^-] + \sqrt{3}\text{Re}[\mathbb{I}_L^-] \right) \end{aligned} \quad (8)$$

where phasors  $\mathbb{I}_L^+$  and  $\mathbb{I}_L^-$  are the positive and negative sequence components of the arc current, respectively, and  $\text{Re}(\cdot)$  and  $\text{Im}(\cdot)$  represent its real and imaginary parts, respectively. Detailed implementation of the SVC control system based on symmetrical components is found in [17].

### III. MULTIVARIABLE COUPLED CONTROL

The control strategy is applied over a SVC structure in order to obtain the firing angles of the thyristors. In this case, the main objective of the controller is to improve the power factor at the PCC, to this end, the angle between the voltage,  $\theta_v$ , and current,  $\theta_i$  at the medium voltage bus (see Fig. 1), is used as input to the controller, as follows:

$$\theta[k] = \theta_v[k] - \theta_i[k] = \begin{bmatrix} \theta_{va}[k] - \theta_{ia}[k] \\ \theta_{vb}[k] - \theta_{ib}[k] \\ \theta_{vc}[k] - \theta_{ic}[k] \end{bmatrix} \quad (9)$$

As output of the controller, a control vector  $\alpha[k]$  is defined as:

$$\alpha[k] = \begin{bmatrix} \alpha_a[k] \\ \alpha_b[k] \\ \alpha_c[k] \end{bmatrix} \quad (10)$$

being  $\alpha[k]$  the firing angle of the SVC at time instant  $t_k = kh$ , being  $k$  the sample and  $h$  the sampling time.

In Fig. 2 is presented the block diagram of the proposed multivariable coupled control of the SVC, for compensate the PF of the distribution electrical system with an electric arc furnace as load. The model of the electric arc is described in Fig. 1.

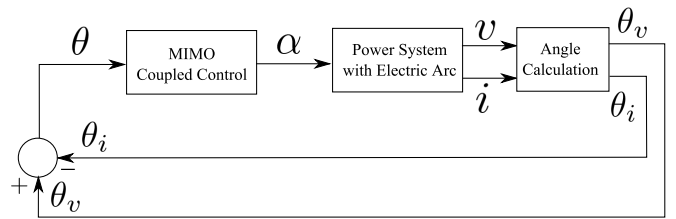


Fig. 2. Block diagram of the Control structure

By considering a multivariable coupled step ahead control based on a polynomial structure [23] and considering the structure proposed in Fig. 2, the following control law is defined based in an ARMA structure:

$$\begin{aligned} \alpha[k] &= P_1\alpha[k-1] + P_2\alpha[k-2] + P_3\alpha[k-3] \\ &+ L_0\theta[k] + L_1\theta[k-1] + L_2\theta[k-2] + L_3\theta[k-3] \end{aligned} \quad (11)$$

where matrices  $P_i \in \mathbb{R}^{3 \times 3}$  and  $L_i \in \mathbb{R}^{3 \times 3}$  contained the parameters of the controller [3], [24]. Equation (11) is rewritten as

$$\alpha[k] = \begin{bmatrix} P_1 & P_2 & P_3 & L_0 & L_1 & L_2 & L_3 \end{bmatrix} \begin{bmatrix} \alpha[k-1] \\ \alpha[k-2] \\ \alpha[k-3] \\ \theta[k] \\ \theta[k-1] \\ \theta[k-2] \\ \theta[k-3] \end{bmatrix} \quad (12)$$

Since the vector  $\alpha[k]$  is computed from past values of  $\alpha$  and from past and present values of  $\theta$ , and considering that matrices  $P_i$  and  $L_i$  are full matrices, the proposed approach can be defined as multivariable coupled control. In addition, a decoupled version of the algorithm could also be obtained if matrices  $P_i$  and  $L_i$  were diagonal matrices.

The design of the controller is performed by considering an off-line estimation of the system with ARMA structure [1], as follows:

$$\begin{aligned} \theta[k] &= B_0\alpha[k] + B_1\alpha[k-1] + B_2\alpha[k-2] + B_3\alpha[k-3] \\ &+ A_1\theta[k-1] + A_2\theta[k-2] + A_3\theta[k-3] \end{aligned} \quad (13)$$

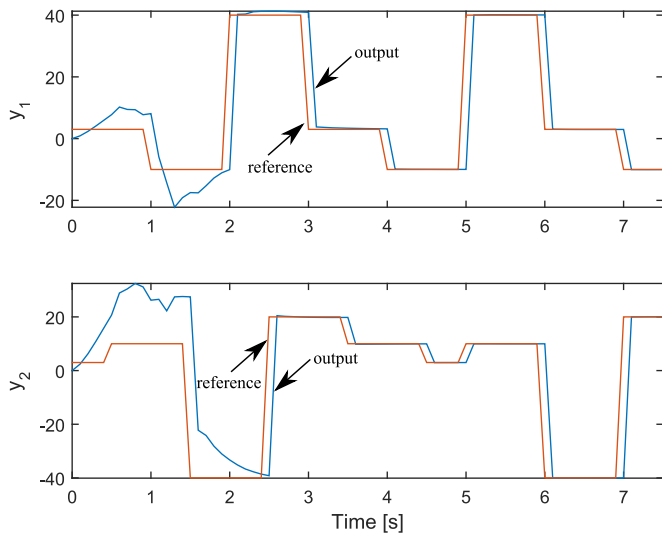


Fig. 3. Reference tracking output for the multivariable coupled system

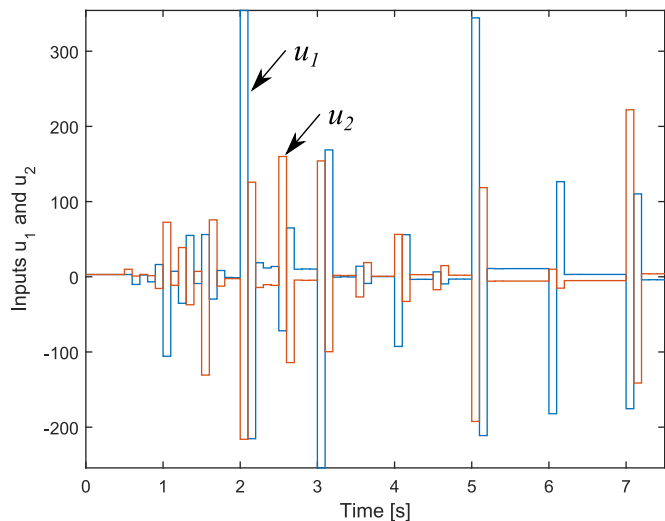


Fig. 4. Control signals for the multivariable coupled system

#### IV. VALIDATION OF THE MULTIVARIABLE ONE STEP AHEAD CONTROL

A validation of the multivariable coupled step ahead control based on the polynomial structure [23] is simulated over a multivariable coupled system defined as:

$$A_1 = \begin{bmatrix} -1.6 & 0.0 \\ 0.0 & -1.6 \end{bmatrix}$$

$$A_2 = \begin{bmatrix} 0.64 & 0.00 \\ 0.00 & 0.64 \end{bmatrix}$$

$$B_0 = \begin{bmatrix} 0.2 & 0.3 \\ 0.1 & 0.5 \end{bmatrix}$$

$$B_1 = \begin{bmatrix} 0.0 & 0.0 \\ 0.0 & 0.0 \end{bmatrix}$$

where the multivariable coupled system is estimated by using an online recursive least square method according to [3]. It is worth noting that the resulting multivariable coupled step ahead control is computed as:

$$u[k] = P_1 u[k-1] + P_2 u[k-2] + L_0 e[k] + L_1 e[k-1] + L_2 e[k-2] \quad (14)$$

being  $e[k] = r[k] - y[k]$  and being  $P_i$  and  $L_i$  defined as follows:

$$P_1 = B_0^{-1}(B_0 - B_1)$$

$$P_2 = B_0^{-1} B_1$$

$$L_0 = B_0^{-1}$$

$$L_1 = B_0^{-1} A_1$$

$$L_2 = B_0^{-1} A_2$$

The references tracking outputs results of the multivariable coupled system by using the multivariable coupled one step ahead control, for a segment of 7.5 seconds with time-varying references, are shown in Fig. 3. The control signals for the reference tracking simulation of Fig. 3 are presented in Fig. 4.

#### V. VALIDATION OF THE PROPOSED SVC CONTROL

A simulation of the system shown in Fig. 1, with the parameters defined in the Appendix is performed. The simulation time is 6.75 seconds, where the controller starts at time 3.375 seconds. The sample time is  $h = 0.0001221$  seconds. A total of 55297 samples is obtained.

The system model that described the dynamic of the electrical power system is estimated by using the ARMA structure of (13), during the first 3.375 seconds, and by considering an offline least squares approach [23]. Once the model parameters are estimated, the controller is computed by using the resulting model parameters. In this case, the obtained control matrices based on a multivariable coupled polynomial control of (11) are the following:

$$P_1 = \begin{bmatrix} 0.94713 & 0.01560 & 0.01491 \\ 0.02159 & 0.95221 & 0.01383 \\ 0.00840 & 0.00780 & 0.93954 \end{bmatrix}$$

$$P_2 = \begin{bmatrix} -0.00040 & -0.001076 & 0.00073 \\ 0.00140 & -0.00089 & -0.00151 \\ 0.00026 & 0.00205 & 0.00064 \end{bmatrix}$$

$$P_3 = \begin{bmatrix} 0.03237 & -0.01931 & 0.01692 \\ 0.01094 & 0.02257 & -0.02463 \\ -0.02083 & 0.01997 & 0.03749 \end{bmatrix}$$

$$L_0 = \begin{bmatrix} -53.23390 & 65.60610 & -0.00055 \\ -158.51985 & -48.18991 & 0.00050 \\ 542.44226 & 209.89234 & 0.00011 \end{bmatrix}$$

$$L_1 = \begin{bmatrix} 190.93379 & -145.32844 & 0.00120 \\ 464.19173 & 105.51994 & -0.00109 \\ -1632.50468 & -656.96284 & -0.00115 \end{bmatrix}$$

$$L_2 = \begin{bmatrix} -218.21551 & 90.21610 & -0.00056 \\ -455.64663 & -62.60510 & 0.00045 \\ 1637.84529 & 685.05691 & 0.00133 \end{bmatrix}$$

$$L_3 = \begin{bmatrix} 80.37489 & -10.32878 & -0.00010 \\ 150.04776 & 5.18593 & -7.1968 \times 10^{-5} \\ -547.66113 & -238.12423 & -0.00024 \end{bmatrix}$$

A comparison analysis is performed among the proposed approach with an ARMA structure and the classical controller based on susceptances control [17] described in (8). In Fig. 5, is presented a 3 seconds segment of the phase A simulation for voltage and current at the PCC, by using the proposed MIMO coupled polynomial control. It can be seen that the time where the controller starts is the time 3.375 seconds.

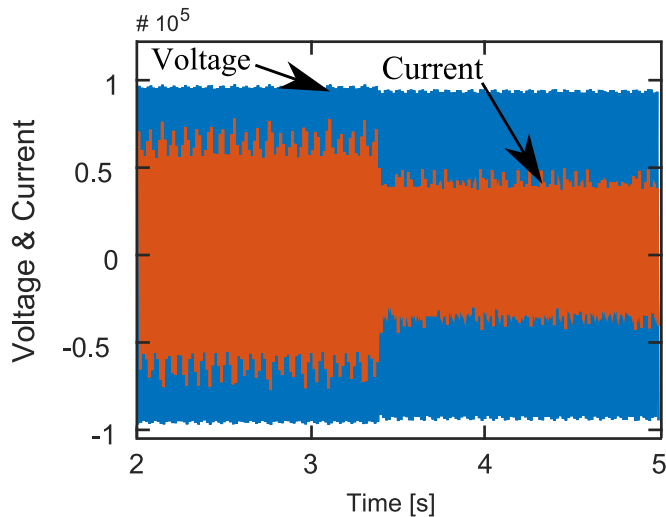


Fig. 5. Simulation 3 seconds segment where the 1-phase voltage and current signals are presented including the uncontrolled and controlled segments

From Fig. 5, a segment of 100 milliseconds of the uncontrolled section is extracted and presented in Fig. 6, where a clear phase shifting is observed for each phase. According to Fig. 15 the observed angles are related to a PF around 0.74.

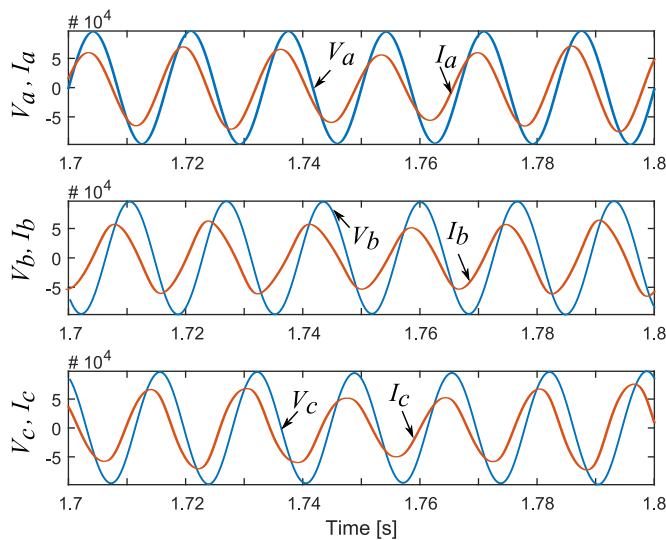


Fig. 6. Voltage and current signals during a 100 milliseconds segment without control

In Fig.8 a three-phase segment of 100 milliseconds showing the voltage and current signals is presented by using the multivariable polynomial approach. It can be seen that in

comparison with the results presented in Fig. 6 the phase angle is reduced.

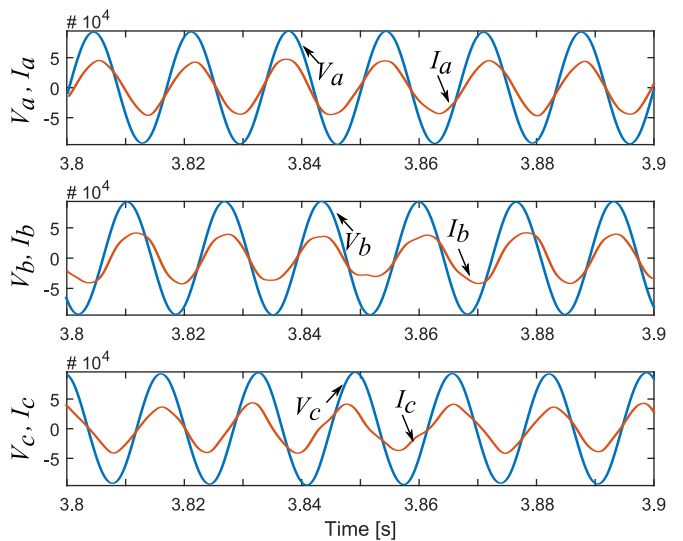


Fig. 7. Voltage and current signals during a 100 milliseconds segment by using the multivariable polynomial approach

As well as in Fig. 7 obtained by the proposed multivariable coupled approach, in Fig. 8 a three-phase segment of 100 milliseconds showing the voltage and current signals is presented by using the classical susceptances control approach. It can be seen that in comparison with the results presented in Fig. 6 the phase angle is also reduced.

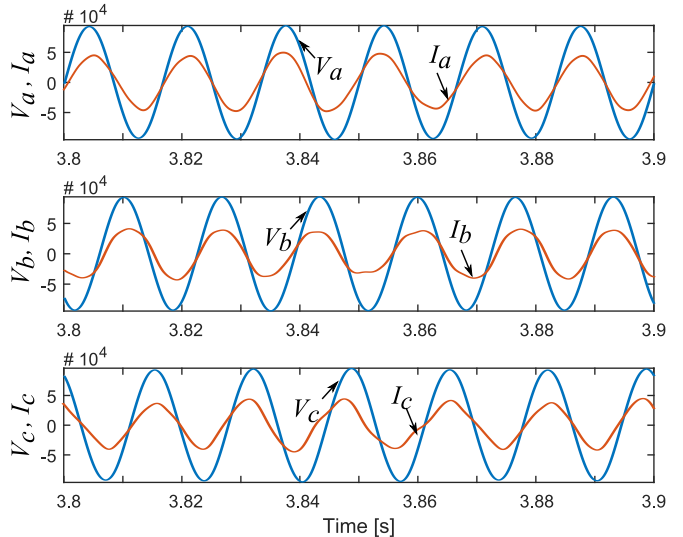


Fig. 8. Voltage and current signals during a 100 milliseconds segment by using the classical control of susceptances

In Fig. 9 the power factor obtained by using the MIMO coupled polynomial control and the classical susceptances control are compared. It can be seen that after the 3.375 seconds an improvement of the PF is obtained for the proposed approach. That can be noticed, since the PF of the proposed approach has higher values than the classical control.

In Fig. 10 are presented the firing angles  $\alpha$  (control signal) applied to the SVC by using the multivariable coupled control.

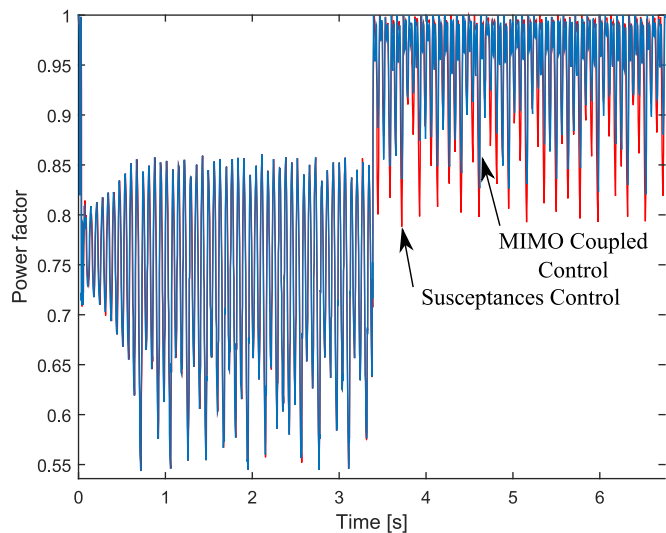


Fig. 9. Power factor controlled by using the multivariable polynomial approach and the susceptance control

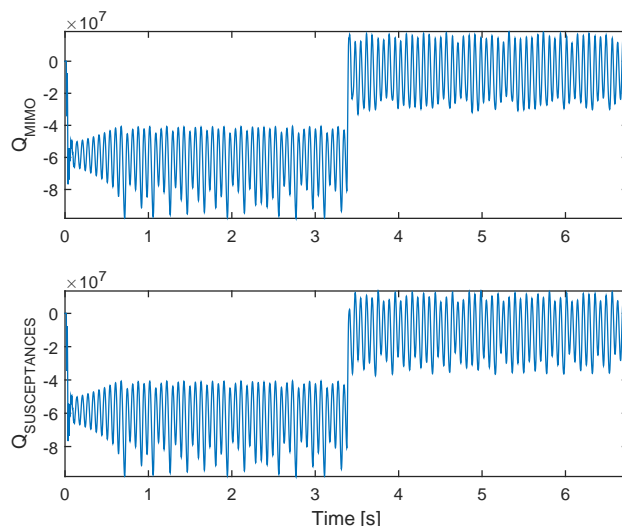


Fig. 11. Reactive power of the fundamental by using the multivariable coupled control

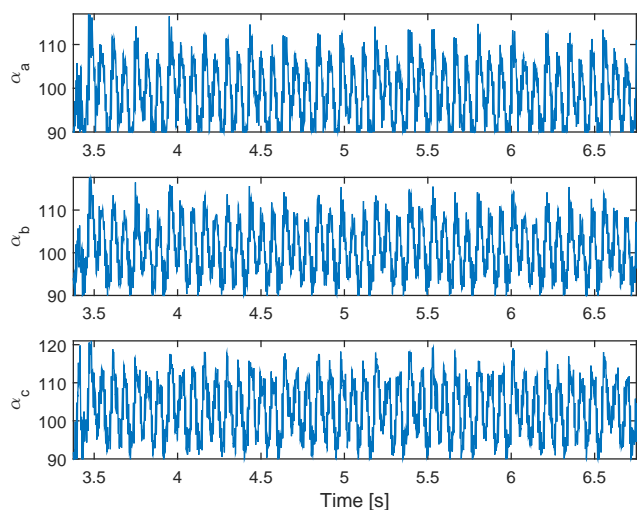


Fig. 10. Firing angles  $\alpha$  applied to the SVC by using the multivariable coupled control

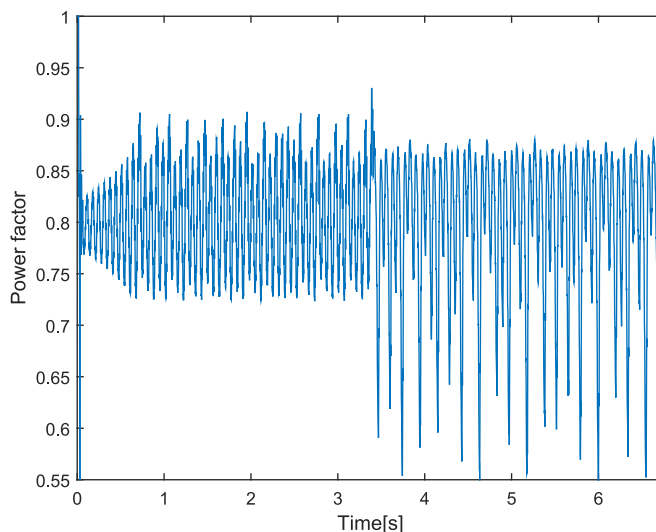


Fig. 12. Power factor at PCC of the electrical power system using an APF.

In Fig. 11 is presented the reactive power during the simulation time with and without control by using the proposed multivariable coupled control.

#### A. Compensation with active power filter

In this subsection are shown the results obtained with an APF to compensate the PF in the electrical power systems shown in Fig. 1. The control system parameters of the APF, used in this work, are described in [22]. In Fig. 12 are shown the PF before and after that the APF is connected to the electric power system. The APF is connected at 0.5 s of the simulation. It can be seen that the PF is not compensated by the APF, and remains in similar values during the whole simulation. Comparing the results of the PF obtained with the SVC (see Fig. 15), the SVC is better than the APF to improve the PF of the electric power system.

In Fig. 13 are shown the Phase A voltage and current signals at the PCC, by using the APF. It is worth noting that the signals are not in phase, in contrast to the SVC-based control system. However, the APF has an advantage over the SVC in the reduction of the harmonic content in the line currents at the PCC as shown in Fig. 14, this due to the inherent nonlinearity of the principle of the operation of the SVC. This advantage of the APF is analyzed in [25] where a shunt hybrid compensator composed by an APC and a SVC is proposed.

In order to clarify the results obtained in Fig. 9 and Fig. 12, a trend line is computed for the corresponding PF. To this end, a mean filter with a 5000 samples window is applied to the PF signals of Fig. 9 and Fig. 12 in order to obtain a trend of the PF evolution. In Fig. 15 it can be seen that the trend of PF obtained after applying the classical susceptances control and the APF are outperformed by the MIMO coupled control.

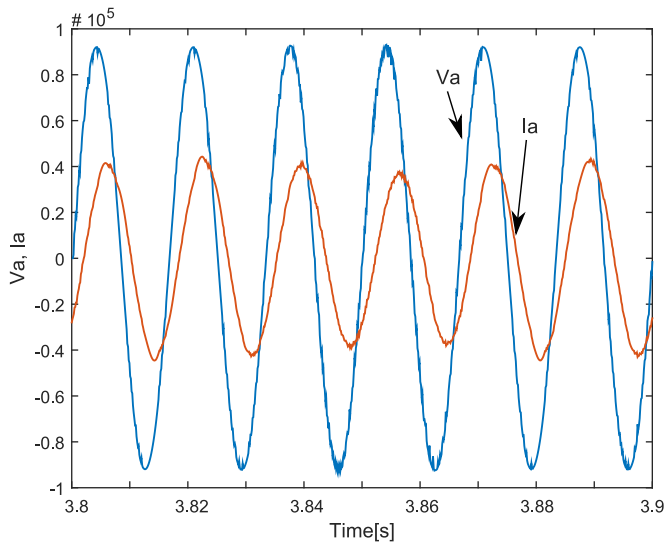


Fig. 13. Voltage and current signal during a 100 milliseconds segment by using an APF.

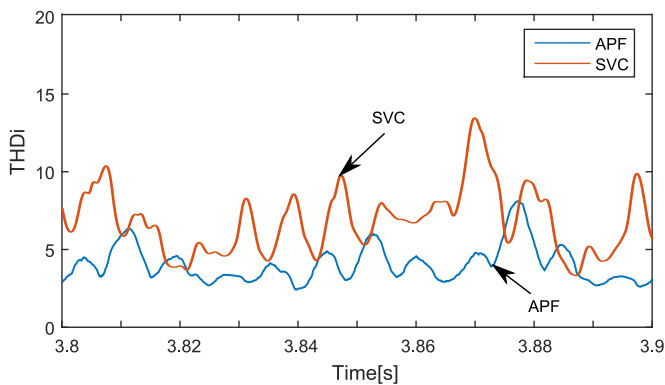


Fig. 14. Comparison of THD in the line current at the PCC, with SVC and APF.

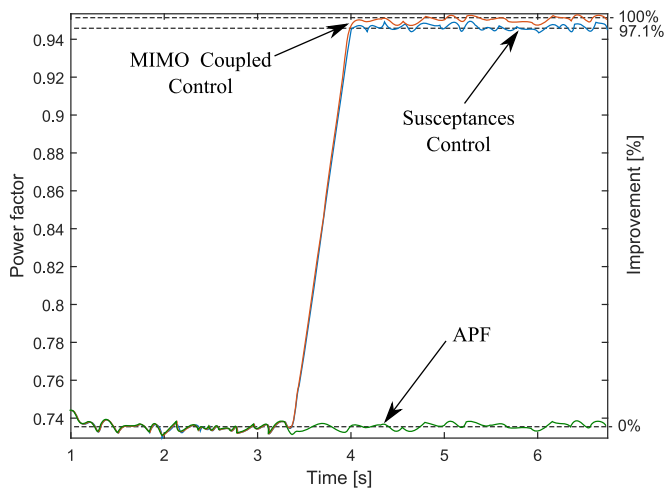


Fig. 15. Power factor controlled trend by using the APF, the multivariable polynomial approach and the susceptances control

In addition, it is worth noting from Fig. 15 that an improvement of 2.9% is achieved for the proposed approach, in comparison with the susceptance control and active filter methods.

## VI. CONCLUSIONS

In this paper, a multivariable polynomial approach is used to design the control of a SVC, to compensate the PF in a distribution system, which include an EAF as a load. The proposed method was compared with the classical susceptances control, and an APF. With the proposed method, the PF increases by 2.9% more than with the classical susceptances control. Based on the results obtained in the PF, the classical susceptances control and the system control of the APF is outperformed by the MIMO coupled control. That can be concluded by analyzing the trend of the PF obtained after applying the MIMO coupled approach. Also, the results obtained show that the SVC allows better compensation in the PF than the APF.

Once the electrical power system model has been estimated by using the ARMA structure, the firing angles of the thyristors have been computed appropriately by the MIMO coupled control, being able to capture the non-linear and time varying nature of the EAF.

As future work, and adaptive control strategy for the SVC can be designed. Also, a multi-objective optimal control considering other functions besides the PF can be considered.

## APPENDIX

Ideal sinusoidal AC voltage source: Line voltage = 115 kV; short circuit power 1960 MVA, X/R ratio = 10.

Transformer  $T_1$ : Three phase  $Y - \Delta_{11}$  (grounded); 80 MVA; 110/20 kV, reactance = 12.5%.

Series reactor at the medium voltage circuit:  $X_L = 98 \text{ m}\Omega$ .

Static VAr compensator (SVC): TCR: Three phase nominal power = 40 MVAR; capacitors bank = -100 MVAR.

Transformer  $T_2$ : Three phase  $Y - \Delta_1$  (grounded); 83 MVA; 20/0.7 kV, reactance = 10%.

Electric arc furnace: 63 MVA, 0.6 kV, 80 kA; low voltage bus resistor  $R_c = 0.38 \text{ m}\Omega$ , electrode reactance  $X_c = 3.23 \text{ m}\Omega$ ; parameters for Eq.(1) phase A:  $k_1 = 3000, k_2 = 10, k_3 = 30$ , phase B:  $k_1 = 2500, k_2 = 10, k_3 = 30$ , phase C:  $k_1 = 4000, k_2 = 10, k_3 = 30$ ; parameters for Chua's circuit for Eq.(3):  $C_1 = 2 \text{ }\mu\text{F}, C_2 = 20 \text{ }\mu\text{F}, L = 3.6 \text{ H}, G = 544.2 \text{ }\mu\text{S}, G_a = -757.576 \text{ }\mu\text{S}, G_b = -409.091 \text{ }\mu\text{S}, E = 1 \text{ V}$ ; modulation index for Eq.(4) phase A:  $w = 0.01$ , phase B  $w = 0.1$ , phase C  $w = 0.14$ .

## REFERENCES

- [1] E. Giraldo, *Multivariable Control*. Germany: Scholar's Press, 2016.
- [2] C. D. Molina-Machado and E. Giraldo, "Bio-inspired control based on a cerebellum model applied to a multivariable nonlinear system," *Engineering Letters*, vol. 28, no. 2, pp. 464-469, 2020.
- [3] F. Osorio-Arteaga, J. J. Marulanda-Durango, and E. Giraldo, "Robust multivariable adaptive control of time-varying systems," *IAENG International Journal of Computer Science*, vol. 47, no. 4, pp. 605-612, 2020.
- [4] B. Singh, K. Al-Haddad, and A. Chandra, "A review of active filters for power quality improvement," *IEEE Transactions on Industrial Electronics*, vol. 46, no. 5, pp. 960-971, 1999.
- [5] A.Soundarrajan, S.Sumathi, and C.Sundar, "Particle swarm optimization based lfc and avr of autonomous power generating system," *IAENG International Journal of Computer Science*, vol. 37, no. 1, pp. 85-92, 2010.
- [6] N. G. K., U. S., and L. Z.V., "Online harmonic elimination of svpwm for three phase inverter and a systematic method for practical implementation," *IAENG International Journal of Computer Science*, vol. 39, no. 2, pp. 220-230, 2012.

- [7] J. Wang, K. Sun, H. Wu, L. Zhang, J. Zhu, and Y. Xing, "Quasi-two-stage multifunctional photovoltaic inverter with power quality control and enhanced conversion efficiency," *IEEE Transactions on Power Electronics*, vol. 35, no. 7, pp. 7073–7085, 2020.
- [8] M. Tanrioven and M. S. Alam, "Modeling, control, and power quality evaluation of a pem fuel cell-based power supply system for residential use," *IEEE Transactions on Industry Applications*, vol. 42, no. 6, pp. 1582–1589, 2006.
- [9] H. Samet, I. Masoudipour, and M. Parniani, "New reactive power calculation method for electric arc furnaces," *Measurement*, vol. 81, no. Supplement C, pp. 251 – 263, 2016.
- [10] M. F. Alves, Z. M. A. Peixoto, C. P. Garcia, and D. G. Gomes, "An integrated model for the study of flicker compensation in electrical networks," *Electric Power Systems Research*, vol. 80, no. 10, pp. 1299 – 1305, 2010.
- [11] E. A. Cano-Plata, A. J. Ustariz-Farfan, and O. J. Soto-Marin, "Electric arc furnace model in distribution systems," *IEEE Transactions on Industry Applications*, vol. 51, no. 5, pp. 4313–4320, Sep. 2015.
- [12] H. Samet, S. Gashtasbi, N. Tashakor, and T. Ghanbari, "Improvement of reactive power calculation in electric arc furnaces utilising kalman filter," *IET Science, Measurement Technology*, vol. 11, no. 3, pp. 241–248, 2017.
- [13] A. Kavousi-Fard, W. Su, T. Jin, A. S. Al-Sumaiti, H. Samet, and A. Khosravi, "A predictive kh-based model to enhance the performance of industrial electric arc furnaces," *IEEE Transactions on Industrial Electronics*, vol. 66, no. 10, pp. 7976–7985, Oct 2019.
- [14] H. Samet and M. Parniani, "Predictive method for improving svc speed in electric arc furnace compensation," *IEEE Transactions on Power Delivery*, vol. 22, no. 1, pp. 732–734, Jan 2007.
- [15] H. Samet and M. E. H. Golshan, "Employing stochastic models for prediction of arc furnace reactive power to improve compensator performance," *IET Generation, Transmission Distribution*, vol. 2, no. 4, pp. 505–515, July 2008.
- [16] T. W. S. Chow and Y. F. Yam, "Measurement and evaluation of instantaneous reactive power using neural networks," *IEEE Transactions on Power Delivery*, vol. 9, no. 3, pp. 1253–1260, July 1994.
- [17] E. Acha, A. Semlyen, and N. Rajakovic, "A harmonic domain computational package for nonlinear problems and its application to electric arcs," *IEEE Transactions on Power Delivery*, vol. 5, no. 3, pp. 1390–1397, July 1990.
- [18] M. P. Kennedy, "Three steps to chaos. i. evolution," *IEEE Transactions on Circuits and Systems I: Fundamental Theory and Applications*, vol. 40, no. 10, pp. 640–656, Oct 1993.
- [19] —, "Three steps to chaos. ii. a chua's circuit primer," *IEEE Transactions on Circuits and Systems I: Fundamental Theory and Applications*, vol. 40, no. 10, pp. 657–674, Oct 1993.
- [20] S. M. M. Agah, S. H. Hosseini, H. A. Abyaneh, and N. Moaddabi, "Parameter identification of arc furnace based on stochastic nature of arc length using two-step optimization technique," *IEEE Transactions on Power Delivery*, vol. 25, no. 4, pp. 2859–2867, Oct 2010.
- [21] O. Ozgun and A. Abur, "Flicker study using a novel arc furnace model," *IEEE Trans. Power Del.*, vol. 17, no. 4, pp. 1158–1163, Oct 2002.
- [22] A. Alzate, A. Escobar, and J. J. Marulanda, "Application of a d-statcom to mitigate arc furnaces power quality problems," in *2011 IEEE Trondheim PowerTech*, 2011, pp. 1–6.
- [23] G. C. Goodwin and K. S. Sin, *Adaptive Filtering, Prediction and Control*. Englewood-Cliffs: Dover Publications Inc., 2009.
- [24] J. S. Velez-Ramirez, M. Bueno-Lopez, and E. Giraldo, "Adaptive control approach of microgrids," *IAENG International Journal of Applied Mathematics*, vol. 50, no. 4, pp. 802–810, 2020.
- [25] M. Torabian Esfahani and B. Vahidi, "Development of optimal shunt hybrid compensator based on improving the measurement of various signals," *Measurement*, vol. 69, pp. 250 – 263, 2015.